Gas Hydrate and Fluid-Related Seismic Indicators Across the Passive and Active Margins off SW Taiwan

14

Liang-Fu Lin, Char-Shine Liu, Christian Berndt, Ho-Han Hsu, Yunshuen Wang, and Song-Chuen Chen

Abstract

Well-constrained and widely distributed bottom simulating reflectors in various geological settings across both passive and active margins make the area offshore southwestern Taiwan an excellent location to study gas hydrate dynamics and fluid flow systems. Seismic data reveal the presence of subsurface fluid flow systems and ubiquitous free gas and gas hydrates. This article aims to summarize and map the different types of seismic observations related to the gas hydrate system. The spatial distribution of seismic indicators for gas accumulation, fluid migration, and the presence of gas hydrates suggests that topographic highs on both passive and active margins are sites of particularly efficient free gas accumulation and gas hydrate formation. Seismic indicators observed in fold and thrust structures suggest that the fluid system in the active margin is structurally controlled and that the highest gas hydrate saturation levels are found in the cores of thrust anticlines on the lower slope of the active margin area.

L.-F. Lin (✉) · C.-S. Liu (✉) · H.-H. Hsu
Ocean Center, National Taiwan University, Taipei, Taiwan
e-mail: linlf@ntu.edu.tw

C.-S. Liu
e-mail: csliu@ntu.edu.tw

C. Berndt
GEOMAR Helmholtz Centre for Ocean Research Kiel, Kiel, Germany

H.-H. Hsu
Institute of Oceanography, National Taiwan University, Taipei, Taiwan

Y. Wang · S.-C. Chen
Central Geological Survey, Ministry of Economic Affairs, Taipei, Taiwan

14.1 Introduction

Gas hydrate investigations offshore SW Taiwan began in the 1990s and blossomed in the 2000s after the initiation of a government-led gas hydrate investigation program that lasted through 2018 (Liu et al. 2006). A comprehensive data set covering gas hydrate system observations has been established over the past 20 years of gas hydrate field investigations. Methods have included 2D and 3D seismic surveys, chirp sonar profiling and side-scan sonar imaging, controlled source electromagnetic surveys, heat flow measurements, OBS surveys, seafloor coring, seafloor filming and photography, high-resolution seafloor mapping and precision sampling in the gas hydrate seepage sites using AUV and ROV, etc. Strong evidence from geological, geophysical, geochemical and biological analytical results suggest that gas hydrates are abundant in both the northeastern South China Sea (SCS) rifted margin (i.e., the passive margin) and in the submarine orogenic wedge (i.e., the active margin) (Liu et al. 2006; Lin et al. 2009a, b; Chen et al. 2017; Berndt et al. 2019). Out of all the data collected, multi-channel seismic reflection (MCS) data has offered the best contributions in understanding the structural geology and stratigraphy for this region. Bottom-simulating reflectors (BSRs) identified on seismic profiles are mapped across both passive and active margins (Fig. 14.1). The continuous and widely distributed BSRs roughly indicate the potential distribution of gas hydrates, and the sub-bottom depth of the BSR has been used to determine the base of gas hydrate stability zone (BGHS) and derive the thermal properties of the margin (Chi et al. 1998; Chen et al. 2014a, b; Kunath et al. 2020). The mapped BSRs suggest that gas hydrates and free gas are present over an area of more than 15,000 km^2 to the south and southwest offshore Taiwan.

To achieve a better understanding of the geological controls on gas hydrate formation, dissociation, and mobilization in an area comprising different tectonic settings and widespread BSRs, a Taiwan-Germany collaborative drilling

J. Mienert et al. (eds.), *World Atlas of Submarine Gas Hydrates in Continental Margins*,
https://doi.org/10.1007/978-3-030-81186-0_14

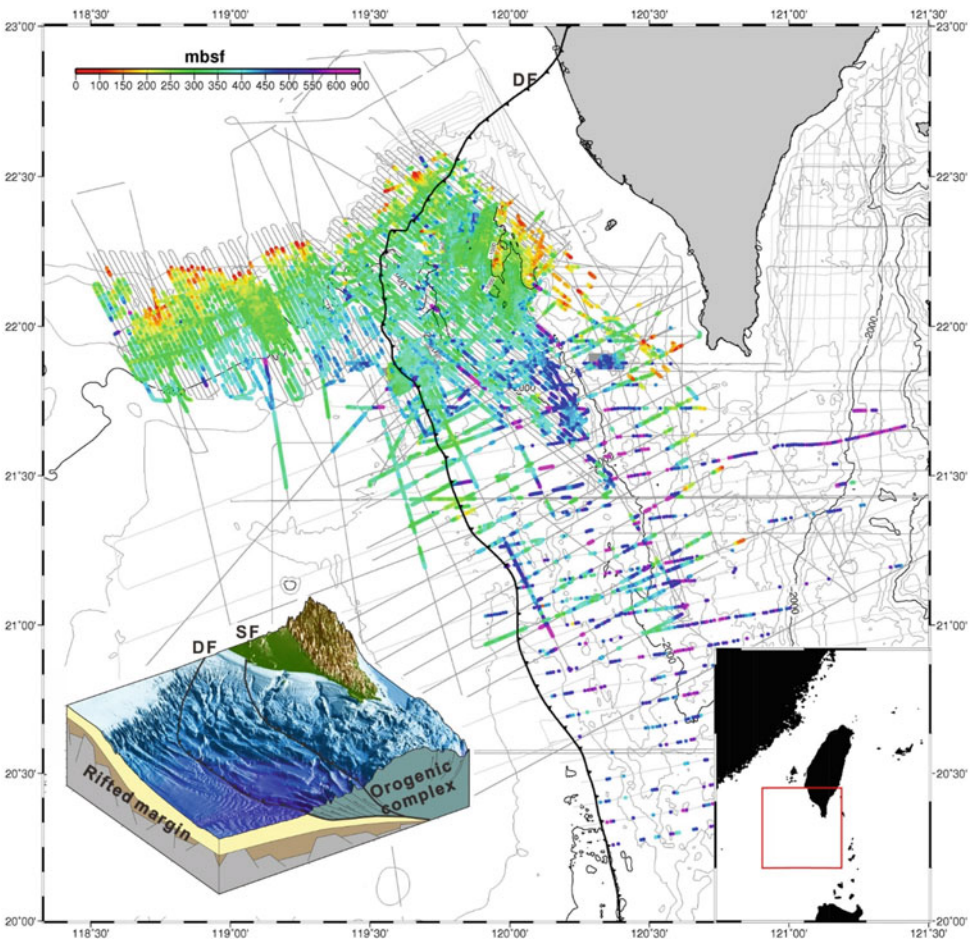

Fig. 14.1 BSR distribution off SW Taiwan. Colors show BSR depth in meters below seafloor (mbsf). Inset lower right, regional setting. Inset lower left, 3D visualization of the tectonic setting. DF, deformation front

project (TaiGer Project) was launched in 2013. The project was carried out using the MeBo200 system, which is designed for core drilling down to 200 mbsf. This shallow drilling was conducted during cruise SO266 on R/V Sonne in both the passive and active margins off SW Taiwan. The analytical results of these cored samples have not yet been published to date. Another notable drilling effort in this area was the GMGS2 expedition conducted by the China Geological Survey (Zhang et al. 2015). The sites investigated throughout this expedition are in the westernmost part of the study area, however, and do not apply to the studies of the systems across the passive and active margins off SW Taiwan. Lacking drilling constraints in this region, the acoustic responses observed in the seismic data become the most important tool for understanding the local gas hydrate and fluid flow systems, as the presence of gas hydrates and free gas alters the physical properties of the sedimentary layers (McConnell et al. 2012; Boswell et al. 2014). These observations not only help to constrain the gas hydrate and fluid systems in the area of interest, but also provide the basis for interpreting the geological and geochemical results of seafloor core sample analyses. A variety of seismic responses related to the gas hydrate and fluid systems observed off SW Taiwan are presented in this article. Interpretations are based on a comprehensive set of geophysical data, the knowledge from conventional petroleum geology, and research on gas hydrates and fluid flow systems in other parts of the world (Bacon et al. 2003; McConnell et al. 2012; Boswell et al. 2014; Nanda 2016). The seismic responses observed across the passive and active margins reveal stark differences in the gas hydrate systems over a small, but tectonically diverse, region.

14.2 Geological Setting

The area offshore SW Taiwan is bound by the rifted SCS margin to its west and the Taiwan orogenic belt to its east (Fig. 14.1). The rifting of the eastern SCS margin began in the late Cretaceous and lasted through the early Oligocene, followed by post-rift sea floor spreading until the late middle-Miocene (Ru and Pigott 1986; Clift and Lin 2001; Taylor and Hayes 2013; Briais et al. 1993; Li et al. 2014). Horsts and grabens formed on the shelf and slope across the continental margin during this period of rifting, and the margin was subsequently buried in a post-rift sedimentary

succession. In the northeastern SCS, the continental margin has been deformed and uplifted since the early middle-Miocene due to the convergent tectonics between the Eurasia Plate and the Philippine Sea Plate. The SCS oceanic crust subducted eastward and formed the Luzon Arc along the western margin of the Philippine Sea Plate (Briais et al. 1993; Yang et al. 1996). During the late Miocene, the Luzon Arc encroached on the northeastern SCS margin, representing the initiation of the arc-continent collision. This was followed by the mountain building processes of the Taiwan orogenesis, which is still ongoing (Teng 1990; Huang et al. 2000).

At present, the deformation front comprising the westernmost compressional structures delineates the boundary between the SCS margin and the orogenic belt (Fig. 14.1) (Bowin et al. 1978; Reed et al. 1992; Liu et al. 1997, 2004). The SCS margin is a tectonically quiet passive margin with some foreland subsidence. A gravity-driven normal faulting system is identified at the shelf edge cutting across the post-rift sediment succession (Lin et al. 2008). In the upper slope of this passive margin, mass wasting features are observed in the shallow strata. These include erosional gullies, gliding surfaces, and mass transport deposits. Shallow strata in the lower slope consist of sediment waves and mass transport deposits, as the transported sediment accumulates at the toe of the slope (Gong et al. 2012, 2015).

To the east of the deformation front, the morphology of the orogenic wedge can be divided into an upper slope domain and a lower slope domain, separated by an escarpment that is related to a splay fault system (or an out-of-sequence thrust, as suggested in earlier studies) (Reed et al. 1992; Liu et al. 1997; Lin et al. 2009a). The lower slope domain is a deep-water fold-and-thrust belt, characterized by folded ridges and piggyback basins. Although the sediment has been deformed, the observed leveed channel systems indicating submarine fan development dominate the shallow strata of the lower slope fold belt (Lin et al. 2016; Lin 2020). The strata in the upper slope domain are poorly imaged due to higher levels of deformation. Diapiric ridges can be identified in this domain, some with mud volcanoes at their peaks (Chen et al. 2014a).

14.3 Seismic Observations

14.3.1 Gas Accumulation

The most common free gas indicator is the BSR. Free gas easily accumulates below the gas hydrate stability zone because the permeability of the strata above is reduced by the formation of gas hydrates. High-amplitude reflectors with reversed polarity are present below the BSR, representing the accumulated free gas (Fig. 14.2a, b, d). The BSRs off SW Taiwan are usually characterized by a strong reflector running roughly parallel to the seafloor, showing reversed polarity in the long-offset multi-channel seismic data, or as the aligned tops of bright spots in the high-resolution seismic data. The results of detailed velocity analyses show high velocity zones above the BSRs and low velocity zones below, especially in the topographic highs where high-amplitude BSRs can be found (e.g., in the erosional remnant ridges on the passive continental slope (Fig. 14.3b; Hsu et al. 2018) and anticlinal or monoclinal ridges in the fold-and-thrust belt (Liu et al. 2006)). This suggests qualitatively that gas accumulates most efficiently beneath topographic highs accompanied by a higher BGHS, where free gas accumulates easily. However, as reflection strength is affected by small variations in the amount of gas, it is not possible to quantify the amount from this seismic attribute alone (Boswell et al. 2014).

Two additional seismic observations corroborate that there are considerable amounts of free gas in the study area. The dominant frequency of the seismic data is reduced below the BSR in some topographic highs, creating a so-called "low-frequency shadow zone" (Fig. 14.2b). This seismic anomaly can be observed below an accumulation of free gas due to preferential absorption of high-frequency seismic energy (Taylor et al. 2000; Cai et al. 2009; Tai et al. 2009; Nanda 2016). The other seismic response is called the "flat spot," which is a direct hydrocarbon indicator widely used in hydrocarbon exploration (Bacon et al. 2003; Nanda 2016). It is usually characterized by a horizontal reflector with a theoretically positive polarity. The occurrence of a flat spot means that the amount of gas present is sufficient to cause gas redistribution according to Archimedes' principle, creating a horizontal gas–water contact in the pores of the sediment. This acoustic impedance contrast between the gas-filled sediment and the pore water-filled sediment constitutes the flat reflector. Flat spots are observed in some of the anticlinal ridges off SW Taiwan (Fig. 14.2b). Both observations indicate that the sediment contains significant amounts of free gas.

14.3.2 Fluid Migration

Two direct seismic indicators for fluid migration that can be observed in the study area are seismic chimneys and faults with reversed polarity reflectors. Seismic chimneys are seismic anomalies related to a fluid pathway. They are typically characterized by chaotic seismic facies in otherwise continuous seismic reflection packages, with reduced seismic amplitudes and a limited lateral extent (Cartwright et al. 2007; Løseth et al. 2011; Karstens and Berndt 2015). It is believed that they are formed by hydro-fracturing, and that they release overpressure. They are one of the most common features observed in areas with active fluid flow. Seismic chimneys can be observed in both the passive and active

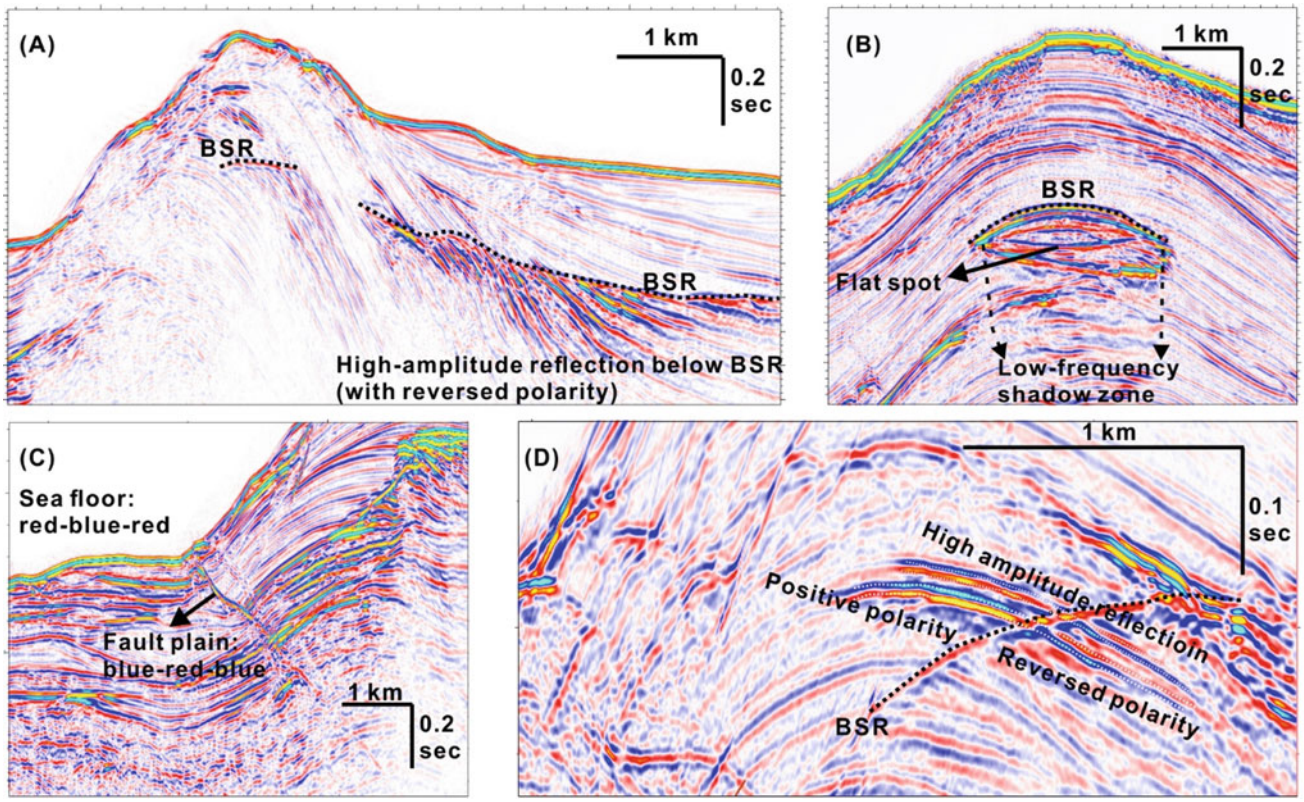

Fig. 14.2 Examples of seismic indicators for the presence of free gas and gas hydrate in the active margin. **a** High-amplitude reversed-polarity reflections below the BSR indicating free gas; **b** flat spot in an anticline where low-frequency shadow zone underneath indicating the presence of free gas; **c** fault plane reflection in reversed polarity at the toe of a thrust anticline; **d** polarity reversal of high-amplitude reflections across BSR indicating concentrated gas hydrate above BSR and free gas below

margins off SW Taiwan, especially at topographic highs (Figs. 14.3c, 14.4). They are mostly rooted at the BSR, revealing their relationship with the over-pressurized, gas-saturated sediments below it. Gas plumes in the seawater, authigenic carbonates, and chemosynthetic communities on the seafloor can be found above these chimneys, indicating that they play an important role in fluid migration.

Most of the thrust faults in the lower slope fold-and-thrust belt are characterized by reflections with reversed polarity, with respect to the seafloor reflection (Fig. 14.2c). The amplitude of these reflections can be strong. Reversed polarity seismic reflections from faults and decollements have been reported at other fold belts and accretionary wedges (Moore et al. 1990, 1995; Bangs and Westbrook 1991; Cochrane et al. 1994; Tobin et al. 1994). The reduced acoustic impedance (i.e., reduction of the product of velocity and density) across faults could be related to porosity changes, dewatering, the presence of gas, or over-pressured pore fluids. These observations may therefore indicate focused fluid flow along the fault planes.

14.3.3 Presence of Gas Hydrate

Gas hydrates can be present in the gas hydrate stability zone wherever there is enough water and free gas. The seismic amplitude from hydrate-bearing sediments generally depends on the hydrate saturation levels of the sediments (McConnell et al. 2012; Boswell et al. 2014). While seismic reflections from massive gas hydrates are rare compared to the observation of BSRs (which are primarily caused by the free gas below gas hydrates), bright spots of positive polarity within the hydrate stability zone may indicate concentrated hydrate accumulations (Fujii et al. 2015). But it is important to note that positive polarity reflections may also be caused by lithological contacts such as sand sheets or carbonate accretions. Therefore, great care must be taken when interpreting gas hydrates from seismic reflection data. Offshore SW Taiwan, there are several seismic amplitude anomalies that may be directly attributed to gas hydrates in the subsurface. They occur mainly in the gas hydrate stability zone directly above the BSR. This setting is much like that of the Nankai trough, which features proven occurrences of gas hydrates (Fujii et al. 2015).

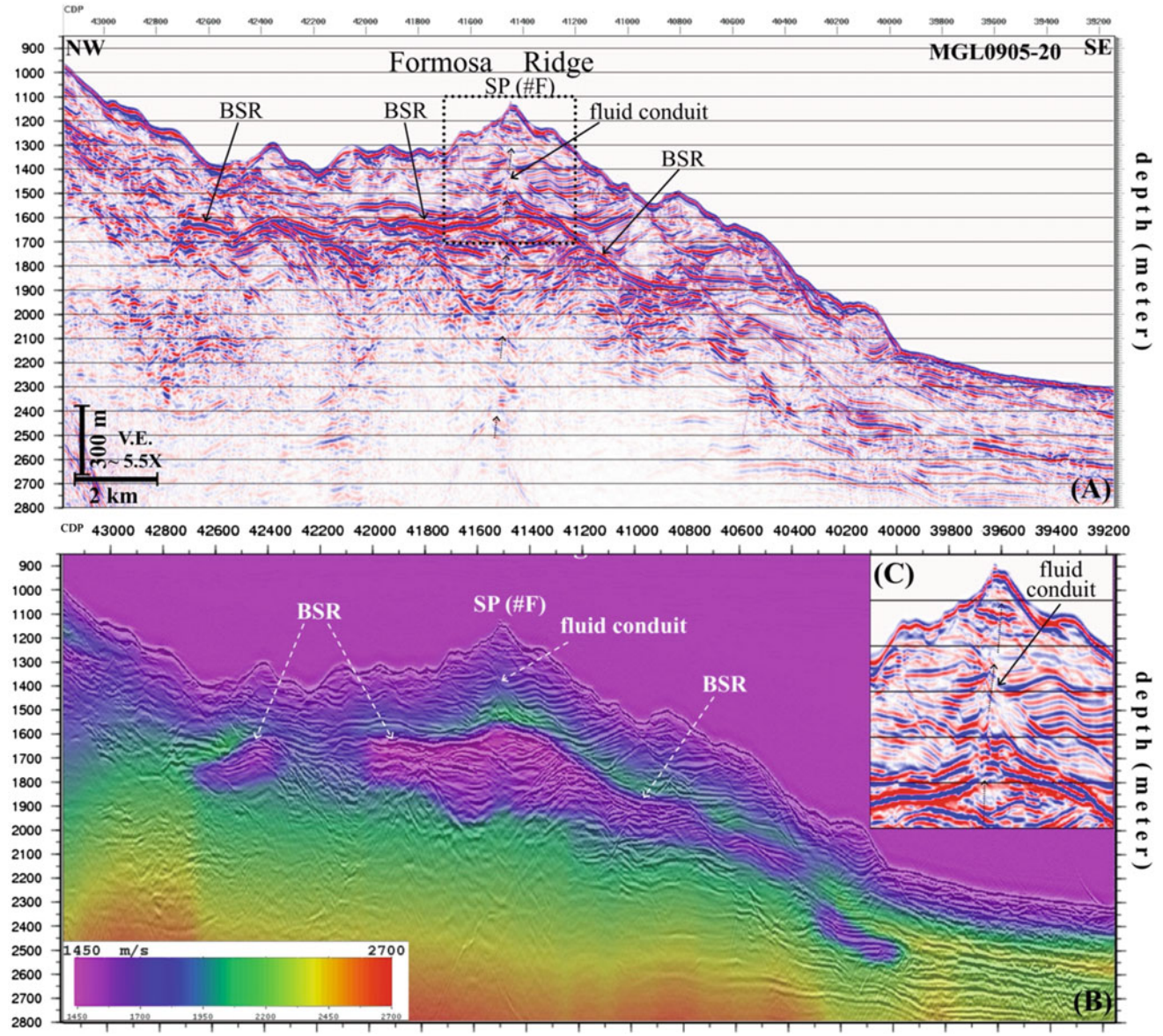

Fig. 14.3 Seismic expression of free gas and gas hydrate in the passive margin (Hsu et al. 2018). **a** Prestack depth migrated image across the Formosa Ridge; **b** corresponding P-wave velocity field showing high velocity anomalies above the BSR and low velocities below; **c** example for a chimney structure below the southern summit of Formosa Ridge (SP (#F) in **a** and **b**

The most important seismic response indicating the presence of hydrate-bearing sediments is the high-amplitude stratal reflector with polarity reversal (i.e., phase shift) crossing the BSR, which indicates the BGHS (Fig. 14.2d). Assuming that the BSR is direct evidence of gas hydrates, the high-amplitude reflections above the BSR may well represent zones of concentrated hydrates (McConnell et al. 2012; Boswell et al. 2014).

There are also high amplitude normal polarity reflections associated with fluid migration pathways (e.g., chimneys, diapirs, crestal fault systems), but it is not clear to what extent they are caused by massive gas hydrates or authigenic carbonate precipitation. Both have been documented by scientific drilling in the SCS (Wang et al. 2017). This association highlights the importance of a free gas supply in the formation of massive hydrate accumulations.

14.4 Distribution of the Seismic Indicators and Implications for Understanding the Hydrate System

Mapping of the seismic indicators discussed in the previous section reveals that their distribution varies across the three tectonic domains of the study area (Fig. 14.4). We find that the topographic highs in both the passive and the active

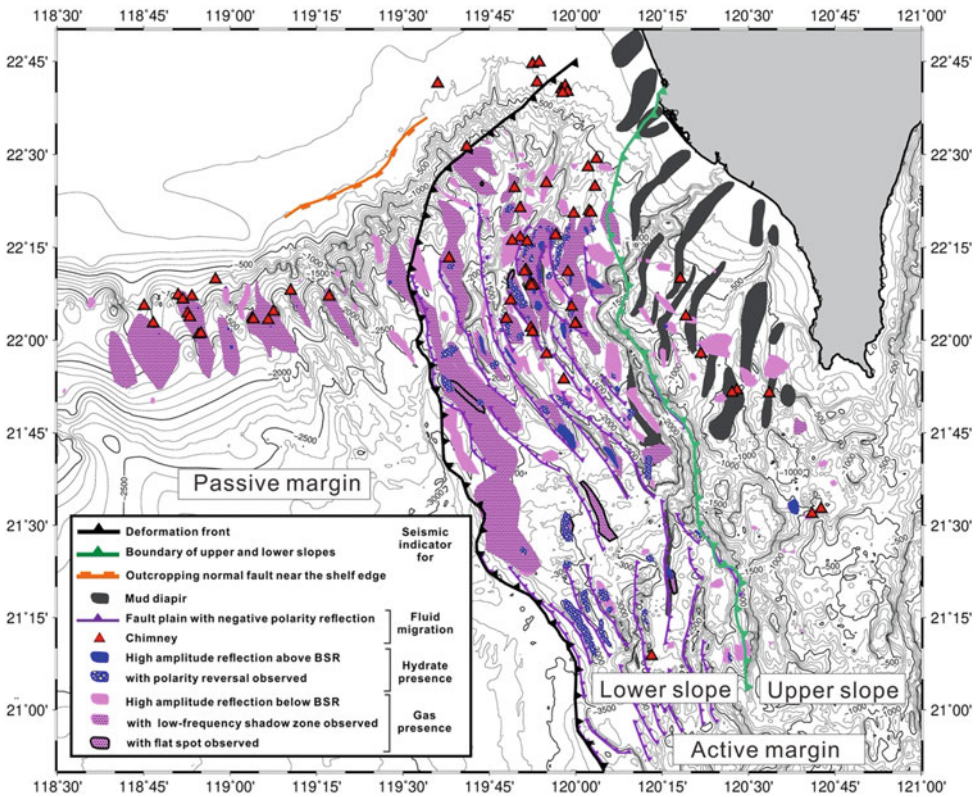

Fig. 14.4 Distribution of gas hydrate and fluid flow related seismic indicators in the study area. 3 tectonic domains from west to east are the passive margin domain, the lower slope domain and the upper slope domain of the active margin

margins are important for free gas accumulation, due to the geometry of the BGHS. These topographic highs are remnants of erosion in the passive margin domain and the anticlinal ridges of the lower slope domain of the active margin, respectively. Seismic chimneys are found underneath the crests of the topographic highs. The association of seismic chimneys and pipes with the crests of topographic highs has been attributed to overpressure build-up within the four-way closure, which is generated by hydrate formation beneath the topographic highs (Bünz et al. 2003) This leads to preferential fluid migration into the gas hydrate stability zone below the highs and even into the water column, controlling the location of chemosynthetic ecosystems (Sibuet and Roy 2003).

In the passive margin domain, the deep-rooted normal fault system cutting across the post-rift succession is proposed to be the main conduit for deep fluid to migrate upward (Lin et al. 2009b). Whereas, in the fold-and-thrust belt of the active margin lower slope domain, an additional fault-controlled fluid migration network has developed. The seismic imaging of the thrust faults in this tectonic domain is characterized by possible fluid-related responses. Although the decollement could potentially serve as a conduit for the collection of deep fluids, no fluid indicator has been observed along the decollement in the lower slope fold-and-thrust belt thus far. On the other hand, a significant accumulation of gas in the fold-and-thrust belt suggests that the dipping strata and thrust faults are important for fluid migration toward the structural highs.

In the upper slope domain of the active margin, the collisional tectonics of the Taiwan orogen have heavily deformed and fragmented the basement, the syn-rift and the post-rift sequences. While this deformation makes them hard to image with seismic data, it also allows for the ascension of deep fluids. The abundant occurrence of mud diapirs, mud volcanoes, and gas plumes in the water column make this fluid migration evident. The fluids that were sampled at the seafloor from the mud volcanos above the mud diapirs contain thermogenic hydrocarbons, proving that they have originated from depth strata (Chuang et al. 2010; Chen et al. 2017). This leakage and the absence of topographic highs may result in less gas accumulation in the upper slope.

The geochemical characteristics of the sediment samples indicate that the natural gases in the passive margin and the lower slope of the active margin are generally biogenic, with little to no thermogenic admixture (Chuang et al. 2010; Chen et al. 2017). Methane fluxes off SW Taiwan are similar to, or slightly greater than, other hydrate provinces (e.g., Blake Ridge and Ulleung Basin) (Borowski et al. 1996; Hong et al. 2013). In addition to the ubiquitous BSR, these results suggest that the shallow sediment contains enough organic matter for substantial biogenic gas production, which fuels the gas hydrate system. The additional thermogenic gas component observed in the upper slope, particularly on top of the interpreted diapiric ridges, may indicate the existence of conventional hydrocarbon systems in the deep parts of the

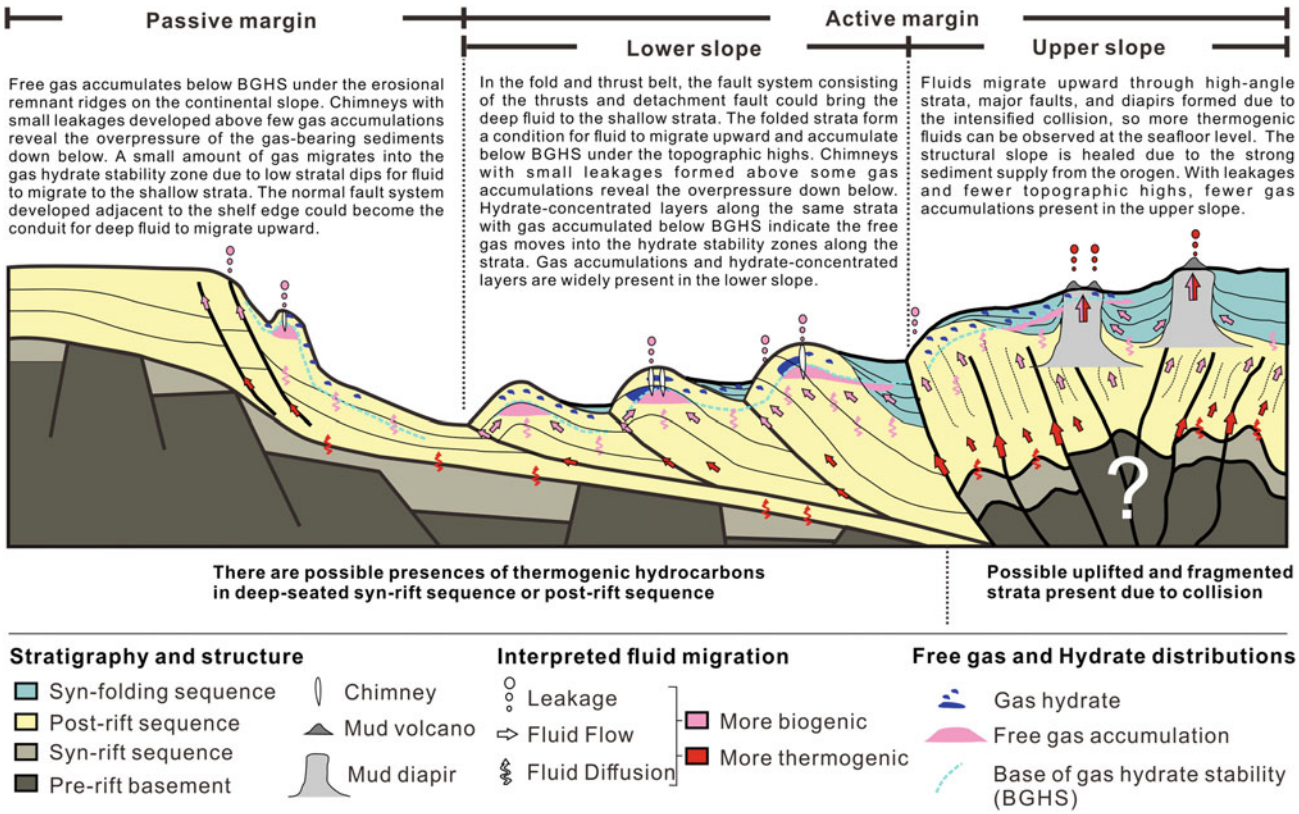

Fig. 14.5 Summary of the various fluid flow and gas hydrate observations along a schematic W-E transect through the active and passive continental margins off SW Taiwan

margin. These could be located in the underlying grabens or in the early post-rift sequence. The presence of two methane sources in the active margin, along with the efficient channeling of methane into the cores of the anticlines by thrust faults and dipping strata, may yield particularly high hydrate concentrations. This is evidenced by the high amplitude reflections found just above the BSRs and supported by high P-wave velocities (Berndt et al. 2019).

14.5 Summary

Various seismic indicators for gas accumulation, fluid migration, and the presence of gas hydrate are observed offshore SW Taiwan (Figs. 14.4 and 14.5). These acoustic responses help to uncover the mechanisms of the fluid and gas hydrate system in the slope areas of both the passive northeastern SCS continental margin and the convergent wedge of the Taiwan orogen. Strong BSRs and many other seismic expressions related to gas hydrates or free gas have been identified, such as gas chimneys, high-amplitude reflections with positive polarity above the BSR or reversed polarity below the BSR, low-frequency shadow zones, flat spots, etc. These indicators suggest that topographic highs, such as the ridges between erosional gullies on the passive margins or the structural ridges in the thrust anticlines on the active margin, control free gas accumulation and gas hydrate formation when free gas enters the gas hydrate stability zone. The fluid flow system in the fold-and-thrust belt is structurally controlled, which is evidenced by the negative polarity reflections along the thrust faults, as well as the observed indications for more gas accumulation and the presence of hydrate-bearing sediment at the structural highs.

The geophysical indications for large amounts of free gas and gas hydrates in the active margin, as well as the geochemical pore water anomalies taken from seafloor core samples, may indicate ongoing petroleum generation in the active margin and fluid migration pathways, starting in the hydrocarbon kitchen and reaching up to the present-day seafloor offshore SW Taiwan.

References

Bacon M, Simm R, Redshaw T (2003) 3-D Seismic Interpretation, 1st edn. Cambridge University Press, Cambridge, UK, p 222

Bangs NLB, Westbrook GK (1991) Seismic modeling of the decollement zone at the base of the Barbados Ridge Accretionary Complex. J Geophys Res Solid Earth 96:3853–3866

Berndt C, Chi W-C, Jegen M et al (2019) Tectonic controls on gas hydrate distribution off SW Taiwan. J Geophys Res Solid Earth 124:1164–1184

Boswell R, Saeki T, Shipp C et al (2014) Prospecting for gas hydrate resources. Methane Hydrate Newslett 14(2):9–15

Borowski WS, Paull CK, Ussler W (1996) Marine pore-water sulfate profiles indicate in situ methane flux from underlying gas hydrate. Geology 24:655–658

Bowin C, Lu RS, Lee C-S et al (1978) Plate Convergence and Accretion in Taiwan-Luzon Region. AAPG Bull 62:1645–1672

Briais A, Patriat P, Tapponnier P (1993) Updated interpretation of magnetic anomalies and seafloor spreading stages in the south China Sea: implications for the Tertiary tectonics of Southeast Asia. J Geophys Res Solid Earth 98:6299–6328

Bünz S, Mienert J, Berndt C (2003) Geological controls on the Storegga gas-hydrate system of the mid-Norwegian continental margin. Earth Planet Sci Lett 209(3–4):291–307

Cartwright J, Huuse M, Aplin A (2007) Seal bypass systems. AAPG Bull 91(8):1141–1166

Cai X, Xu T-J, Tang J-M et al (2009) Research and application of gas detection techniques using full-wave attributes in southwest China. First Break 27(11):91–96

Chen S-C, Hsu S-K, Wang Y et al (2014a) Distribution and characters of the mud diapirs and mud volcanoes off southwest Taiwan. J Asian Earth Sci 92:201–214

Chen L, Chi W-C, Wu S-K et al (2014b) Two dimensional fluid flow models at two gas hydrate sites offshore southwestern Taiwan. J Asian Earth Sci 92:245–253

Chen N-C, Yang TF, Hong W-L et al (2017) Production, consumption, and migration of methane in accretionary prism of southwestern Taiwan. Geochem Geophys 18:2970–2989

Chi W-C, Reed DL, Liu C-S et al (1998) Distribution of the bottom-simulating reflector in the offshore Taiwan collision zone. Terrestrial, Atmospheric and Oceanic Sciences 9(4):779–794

Chuang P-C, Yang TF, Hong W-L et al (2010) Estimation of methane flux offshore SW Taiwan and the influence of tectonics on gas hydrate accumulation. Geofluids 10:497–510

Clift P, Lin J (2001) Preferential mantle lithospheric extension under the South China margin. Mar Pet Geol 18:929–945

Cochrane GR, Moore JC, MacKay ME et al (1994) Velocity and inferred porosity model of the Oregon accretionary prism from multichannel seismic reflection data: Implications on sediment dewatering and overpressure. J Geophys Res Solid Earth 99:7033–7043

Fujii T, Suzuki K, Takayama T et al (2015) Geological setting and characterization of a methane hydrate reservoir distributed at the first offshore production test site on the Daini-Atsumi Knoll in the eastern Nankai Trough, Japan. Mar Pet Geol 66:310–322

Gong C, Wang Y, Peng X et al (2012) Sediment waves on the South China Sea Slope off southwestern Taiwan: implications for the intrusion of the Northern Pacific Deep Water into the South China Sea. Mar Pet Geol 32:95–109

Gong C, Wang Y, Xu S et al (2015) The northeastern South China Sea margin created by the combined action of down-slope and along-slope processes: processes, products and implications for exploration and paleoceanography. Mar Pet Geol 64:233–249

Hong W-L, Torres ME, Kim J-H et al (2013) Carbon cycling within the sulfate-methane-transition-zone in marine sediments from the Ulleung Basin. Biogeochemistry 115:129–148

Hsu HH, Liu CS, Morita S, Tu SL, Lin S, Machiyama H, Azuma W, Ku CY, Chen SC (2018) Seismic imaging of the Formosa Ridge cold seep site offshore of southwestern Taiwan. MarineGeophys Res 39(4) 523–535. https://doi.org/10.1007/s11001-017-9339-y

Huang C-Y, Yuan PB, Lin C-W et al (2000) Geodynamic processes of Taiwan arc–continent collision and comparison with analogs in Timor, Papua New Guinea, Urals and Corsica. Tectonophysics 325:1–21

Karstens J, Berndt C (2015) Seismic chimneys in the Southern Viking Graben—implications for palaeo fluid migration and overpressure evolution. Earth Planet Sci Lett 412(C):88–100

Kunath P, Chi W-C, Berndt C et al (2020) A shallow seabed dynamic gas hydrate system off SW Taiwan: Results from 3-D seismic, thermal, and fluid migration analyses. J Geophys Res Solid Earth 125(11):e2019JB019245-T

Li C-F, Xu X, Lin J et al (2014) Ages and magnetic structures of the South China Sea constrained by deep tow magnetic surveys and IODP Expedition 349. Geochem Geophys 15:4958–4983

Lin L-F (2020) Depositional elements and seismic characteristics of the Penghu ang Gaoping submarine fan systems off SW Taiwan. National Taiwan University. PhD dissertation, 131 pp

Lin AT, Liu CS, Lin CC, Schnurle P, Chen GY, Liao WZ, Teng LS, Chuang HJ, Wu MS (2008) Tectonic features associated with the overriding of an accretionary wedge on top of a riftedcontinental margin: an example from Taiwan. Marine Geology 255(3–4):186–203. https://doi.org/10.1016/j.margeo.2008.10.002

Lin AT, Yao B, Hsu S-K et al (2009a) Tectonic features of the incipient arc-continent collision zone of Taiwan: implications for seismicity. Tectonophysics, Arc-Continent Collision 479:28–42

Lin C-C, Tien-Shun Lin A, Liu C-S et al (2009b) Geological controls on BSR occurrences in the incipient arc-continent collision zone off southwest Taiwan. Mar Pet Geol 26:1118–1131

Lin L-F, Liu C-S, Lin C-C et al (2016) Geological characteristics and fluid-related seismic signals in Lower Gaoping Slope, offshore Southwestern Taiwan. Central Geol Surv Spec Pub 30:159–180 (in Chinese with English abstract)

Liu C-S, Huang IL, Teng LS (1997) Structural features off southwestern Taiwan. Mar Geol 137:305–319

Liu C-S, Deffontaines B, Lu CY et al (2004) Deformation patterns of an accretionary wedge in the transition zone from subduction to collision offshore southwestern Taiwan. Mar Geophys Res 25:123–137

Liu C-S, Schnurle P, Wang Y, San-Hsiung C, Song-Chuen C, Hsiuan TH (2006) Distributionand characters of gas hydrate offshore of southwestern Taiwan. Terrestr Atmospheric Ocean Sci 17(4) 615. https://doi.org/10.3319/TAO.2006.17.4.615(GH)

Liu C-S, Schnurle P, Wang Y et al (2006) Distribution and characters of gas hydrate offshore of southwestern Taiwan. TAO Terr Atmos Oceanic Sci 17:615

Løseth H, Wensaas L, Arntsen B et al (2011) 1000m long gas blow-out pipes. Mar Pet Geol 28(5):1047–1060

McConnell DR, Zhang Z, Boswell R (2012) Review of progress in evaluating gas hydrate drilling hazards. Mar Petr Geol 34(1):209–223

Moore GF, Shipley TH, Stoffa PL et al (1990) Structure of the Nankai Trough Accretionary Zone from multichannel seismic reflection data. J Geophys Res Solid Earth 95:8753–8765

Moore JC, Moore GF, Cochrane GR et al (1995) Negative-polarity seismic reflections along faults of the Oregon accretionary prism: indicators of overpressuring. J Geophys Res Solid Earth 100:12895–12906

Nanda NC (2016) Seismic data interpretation and evaluation for hydrocarbon exploration and production: a practitioner's guide. Springer

Reed DL, Lundberg N, Liu C-S et al (1992) Structural relations along the margins of the offshore Taiwan accretionary wedge: implications for accretion and crustal kinematics. Acta Geological Taiwanica 105–122

Ru K, Pigott JD (1986) Episodic rifting and subsidence in the South China Sea. AAPG Bull 70:1136–1155

Sibuet M, Roy KO-L (2003) Cold seep communities on continental margins: structure and quantitative distribution relative to geological and fluid venting patterns. In: Sea change. Berlin, Heidelberg, Springer, pp 235–251

Tai S, Puryear C, Castagna JP (2009) Local frequency as a direct hydrocarbon indicator. SEG Tech Prog Expand Abstr 28:2160–2164

Taylor B, Hayes DE (2013) Origin and history of the South China Sea Basin. In: The Tectonic and geologic evolution of Southeast Asian Seas and Islands: Part 2. American Geophysical Union (AGU), pp 23–56

Taylor MH, Dillon WP, Pecher IA (2000) Trapping and migration of methane associated with the gas hydrate stability zone at the Blake Ridge Diapir: new insights from seismic data. Mar Geol 164(1–2):79–89

Teng LS (1990) Geotectonic evolution of late Cenozoic arc-continent collision in Taiwan. Tectonophysics, Geodynamic Evolution of the Eastern Eurasian Margin 183:57–76

Tobin HJ, Moore JC, Moore GF (1994) Fluid pressure in the frontal thrust of the Oregon accretionary prism: experimental constraints. Geology 22:979–982

Wang X, Liu B, Qian J et al (2017) Geophysical evidence for gas hydrate accumulation related to methane seepage in the Taixinan Basin, South China Sea. J Asian Earth Sci 168:27–37

Yang TF, Lee T, Chen C-H et al (1996) A double island arc between Taiwan and Luzon: consequence of ridge subduction. Tectonophysics 258:85–101

Zhang G, Liang J, Yang S et al (2015) Geological features, controlling factors and potential prospects of the gas hydrate occurrence in the east part of the Pearl River Mouth Basin, South China Sea. Mar Pet Geol 67:356–367